



Published in final edited form as:

*Ophthalmic Surg Lasers Imaging*. 2009 ; 40(1): 25–31.

## Comparison of StratusOCT and Cirrus HD-OCT Imaging in Macular Diseases

**Peter M. Brennen, MD, Larry Kagemann, MS, and Thomas R. Friberg, MD**

From the UPMC Eye Center (PMB, LK, TRF), Department of Ophthalmology, University of Pittsburgh School of Medicine, Pittsburgh; and the Department of Bioengineering (LK), Swanson School of Engineering, University of Pittsburgh, Pittsburgh, Pennsylvania

### Abstract

**BACKGROUND AND OBJECTIVE**—The Cirrus HD-OCT (Carl Zeiss Meditec, Dublin, CA) device is a spectral-domain optical coherence tomography system that allows faster data acquisition than the previous generation StratusOCT (Carl Zeiss Meditec, Dublin, CA), which is a time-domain device. The authors compared images from both units to determine the clinical usefulness of spectral-domain optical coherence tomography technology in patients with macular diseases.

**PATIENTS AND METHODS**—Six consecutive patients were imaged with both the Cirrus HD-OCT and the StratusOCT devices and the images were compared.

**RESULTS**—Cirrus HD-OCT images were typically more useful than StratusOCT images for assessing fine architectural details in macular pathology. The Cirrus HD-OCT software also facilitated a better understanding of three-dimensional data volumes.

**CONCLUSIONS**—Commercially available spectral-domain optical coherence tomography is a clinically useful tool for visualizing and understanding macular diseases and offers benefits not inherent in previous generation machines.

### INTRODUCTION

Optical coherence tomography (OCT)<sup>1</sup> has been used in a wide range of biomedical applications.<sup>2,3</sup> OCT noninvasively acquires high-resolution, cross-sectional images of the retina,<sup>4</sup> aiding in the diagnosis and monitoring of various macular diseases.<sup>5</sup> The StratusOCT device (Carl Zeiss Meditec, Dublin, CA) is a commercially available time-domain OCT system capable of acquiring OCT reflectivity data at a rate of 400 axial scans per second. A spectral-domain OCT (SD-OCT) system, Cirrus HD-OCT (Carl Zeiss Meditec) recently gained U.S. Food and Drug Administration approval. SD-OCT technology improves on time-domain systems, allowing performance of up to 27,000 axial scans per second.<sup>6,7</sup> The increased axial scan rate results in approximately 50 times faster data acquisition in practice.

We obtained images with both StratusOCT and Cirrus HD-OCT systems from a representative group of patients with macular diseases with the aim of determining the clinical usefulness of a commercially available SD-OCT system in an environment where a time-domain system is already widely used.

---

Address correspondence to Thomas R. Friberg, MD, UPMC Eye Center, 203 Lothrop Street, Suite 824, Pittsburgh, PA 15213.  
The authors have no financial or proprietary interests in the materials presented herein.

## PATIENTS AND METHODS

All procedures were approved by the institutional review board at the University of Pittsburgh and informed consent was provided by the subjects before participation in the studies. The study was performed in compliance with the tenets of the Declaration of Helsinki and the Health Insurance Portability and Accountability Act.

Six consecutive patients with diabetic macular edema, exudative age-related macular degeneration, or vitreomacular traction were imaged with both StratusOCT and Cirrus HD-OCT systems on the same day. For StratusOCT imaging, the Macular Thickness Map scan protocol was used. The protocol consists of 6 linear scans in a spoke pattern separated by 30° intervals centered at the fovea. The line scans were 6 mm in the transverse direction, had a 2-mm axial depth, and were composed of 512 axial scans each. For Cirrus HD-OCT imaging, the Macular Cube 200 × 200 Combo protocol was used. The protocol consists of two perpendicular line scans centered at the fovea followed by a cube scan also centered at the fovea. The line scans were 6 mm in the transverse direction, had a 2-mm axial depth, and were composed of 1,000 axial scans each. The cube scan was 6 × 6 mm, had a 2-mm axial depth, and was composed of 200 × 200 axial scans.

Because the Cirrus HD-OCT protocol only captures two high-resolution line scans, the inferior to superior and temporal to nasal (right eye) and nasal to temporal (left eye) line scans of the StratusOCT were compared with the corresponding line scans obtained from the Cirrus HD-OCT. Best efforts were made to obtain the highest quality scans using both modalities. The cube scan data were manipulated with the Cirrus HD-OCT software to provide additional information as deemed necessary. Internal limiting membrane and retinal pigment epithelium segmentation were performed on the cube scan data to provide three-dimensional maps of the internal limiting membrane and retinal pigment epithelium.

We used the advanced visualization component of the software to average axial scan reflectivity values over a user-defined distance at a given axial depth in the cube scan data to present two-dimensional or “C-scan” images. When combined with internal limiting membrane and retinal pigment epithelium segmentation, this system enabled averaging of reflectivity values based on a contour dictated by segmentation results, effectively compensating for retinal pigment epithelium or internal limiting membrane curvature. The resulting C-scan images were aligned to the retinal pigment epithelium or internal limiting membrane as identified by the segmentation algorithm. When indicated as part of the clinical workup, optomap *fa* (Optos, Marlborough, MA) fundus photographs and fluorescein angiography were obtained.

## RESULTS

### Case 1: Diabetic Macular Edema and Serous Retinal Detachment

A 68-year-old woman with diabetic maculopathy in both eyes underwent StratusOCT and Cirrus HD-OCT imaging 3 months after grid laser therapy in the right eye. Late-phase optomap *fa* fluorescein angiography of the right eye showed diffuse leakage in the foveal area (Fig. 1A). Cirrus HD-OCT images defined the architecture of cystoid changes with greater clarity than StratusOCT (Figs. 1B and 1C). Neither modality is able to clearly demonstrate preservation of the photoreceptor layer architecture in the area of serous retinal detachment. Advanced visualization defines the two-dimensional extent of the detachment in a single image (Fig. 1D).

### **Case 2: Massive Subretinal Fluid Due to Exudative Age-Related Macular Degeneration**

An 85-year-old man with a history of exudative age-related macular degeneration in both eyes and recent worsening of visual acuity in the left eye underwent StratusOCT and Cirrus HD-OCT imaging as part of an evaluation for anti-vascular endothelial growth factor therapy. Both modalities demonstrated disciform scar and massive subretinal fluid accumulation in the left eye. Cirrus HD-OCT shows portions of the outer nuclear layer still adhering to scarred areas, a finding difficult to appreciate with StratusOCT (Figs. 2A and 2B). The cystoid structures are more clearly defined with Cirrus HD-OCT when compared with the StratusOCT. The internal limiting membrane map obtained from the Cirrus HD-OCT macular thickness analysis used shadowing to express the three-dimensional appearance of internal limiting membrane segmentation data (Fig. 2C).

### **Case 3: Diabetic Macular Edema**

A 79-year-old woman with a history of nonproliferative diabetic retinopathy and diabetic macular edema in the right eye underwent StratusOCT and Cirrus HD-OCT imaging. Both StratusOCT and Cirrus HD-OCT images (Figs. 3A and 3B) demonstrated persistent macular edema after earlier anti-vascular endothelial growth factor treatment, and the decision was made to proceed with continued intravitreal therapy. Both modalities show cystoid structures. Cirrus HD-OCT clearly defines the deeper borders of the large central cavity.

Additionally, Cirrus HD-OCT shows gross preservation of the external limiting membrane and photoreceptor inner segment/outer segment in the fovea. With StratusOCT, the external limiting membrane is not seen and the photoreceptor layers are not well visualized in the central fovea. Advanced visualization (Fig. 3C) shows the two-dimensional configuration of multiple hard exudates noted on prior ophthalmoscopic examination.

### **Case 4: Severe Vitreomacular Traction**

A 74-year-old man with a history of epiretinal membrane and mild vitreomacular traction in the right eye complained of worsening visual acuity in the right eye. Cirrus HD-OCT and StratusOCT imaging show severe vitreomacular traction (Figs. 4A and 4B). The architecture of foveal cysts and spacing of retinal folds are seen more clearly with Cirrus HD-OCT when compared with StratusOCT. Sharp vitreomacular attachment points can be identified in the Cirrus HD-OCT images. Advanced visualization suggests that the tractional force is centered in the superior macula (Fig. 4C). This corresponds well with the direction of traction seen in individual slice images from both Cirrus HD-OCT and StratusOCT. Note the presence of foveal cysts in the same advanced visualization image.

### **Case 5: Extensive Choroidal Neovascularization Due to Exudative Age-Related Macular Degeneration**

An 83-year-old man complained of reduced visual acuity in the right eye and on ophthalmoscopic examination of the right eye was found to have a subretinal hemorrhage (Fig. 5A). Late-phase optomap *fa* fluorescein angiography (Fig. 5B) of the right eye demonstrated central hyperfluorescence surrounded by a hemorrhage blockage consistent with an active choroidal neovascular membrane. Cirrus HD-OCT and StratusOCT imaging demonstrated extensive choroidal neovascularization and adjacent subretinal fluid (Figs. 5C and 5D). Cirrus HD-OCT images allowed identification of the intact external limiting membrane in the inferior section of the image, macular edema in the central section, and a small pocket of subretinal fluid adjacent to the choroidal neovascular membrane in the superior section. StratusOCT images did not clearly demonstrate these findings.

### Case 6: Exudative Age-Related Macular Degeneration With Disciform Scar

An 84-year-old man with a history of nonexudative age-related macular degeneration in both eyes complained of reduced visual acuity in the left eye and was found to have a central disciform scar with subretinal fluid and hemorrhage in the left eye on ophthalmoscopic examination (Fig. 6A). Late-phase optomap *fa* fluorescein angiography demonstrated a central area of hyperfluorescence consistent with an active choroidal neovascular membrane (Fig. 6B). Cirrus HD-OCT and StratusOCT imaging demonstrate an extensive epiretinal membrane, cystoid edema, and scarring (Figs. 6C and 6D). Cirrus HD-OCT images provided superior resolution for evaluation of the architecture of both the epiretinal membrane and cystoid edema when compared with StratusOCT. Advanced visualization demonstrates deep retinal folds induced by the epiretinal membrane (Fig. 6E).

## DISCUSSION

We found that in a small consecutive series of eyes with macular disease, Cirrus HD-OCT rendered pathologic findings with greater detail than StratusOCT. Additionally, preservation of normal retinal structure was easier to assess using Cirrus HD-OCT. Both the improved resolution and higher axial scan acquisition rate of the Cirrus HD-OCT contributed to our understanding of disease morphology and intraretinal layer relationships.

The Cirrus HD-OCT system achieves approximately double the axial resolution of the previous generation StratusOCT device. Cirrus HD-OCT is capable of 5- $\mu$ m axial and 15- $\mu$ m transverse resolution in tissue and StratusOCT is capable of 8- to 10- $\mu$ m axial and approximately 20- $\mu$ m transverse resolution in tissue. In our opinion, the increased resolution allowed superior visualization of the external limiting membrane and photoreceptor inner segment/outer segment with Cirrus HD-OCT. The enhanced visualization of these layers may be useful in assessing external limiting membrane disruption and photoreceptor loss in a variety of pathologies. Appreciation of small cystoid structures was also easier and the microarchitecture of cystoid edema was rendered with greater detail.

It is important to note that when comparing different imaging modalities, it is impossible to ensure that scans are obtained from exactly the same areas of interest. It is likely that some subtle findings observed with Cirrus HD-OCT may not be identified in StratusOCT images and vice versa due to fixation loss or physiologic eye movements.

Motion artifacts interfere with the identification of subtle morphologic features and can contribute to segmentation algorithm failure. The higher axial scan acquisition rate of the Cirrus HD-OCT system allows for reduction of motion artifacts in line scans and rapid acquisition of three-dimensional data volumes. The Cirrus HD-OCT software presents three-dimensional data volumes and segmentation results in the form of interactive internal limiting membrane and retinal pigment epithelium maps, fundus image overlays, and an advanced visualization system that allowed rapid interpretation of the three-dimensional data. The use of three-dimensional data has the potential to facilitate clinician and patient understanding of disease processes.

The current study does not address whether the increased speed and resolution of the Cirrus HD-OCT device significantly improves the global diagnostic performance of OCT imaging, nor does it identify specific instances where therapeutic decisions were influenced by the additional information obtained. Larger, disease-specific studies are needed to evaluate the frequency with which Cirrus HD-OCT allows identification of pathology not visible with StratusOCT or leads to changes in therapeutic course.



Experimental OCT technology continues to progress quickly toward the goal of in vivo, cellular resolution imaging of the retina. A recent study showed the utility of imaging macular pathologies using ultrahigh-resolution OCT compared with the StratusOCT.<sup>8</sup> We believe that Cirrus HD-OCT is capable of providing a similar, that albeit less dramatic, advantage over StratusOCT. Although ultrahigh-resolution and high-speed ultrahigh-resolution OCT systems are expensive and limited to experimental use,<sup>8–11</sup> lower resolution SD-OCT systems with current commercial availability, such as Cirrus HD-OCT, are a clinically useful tool that can be implemented today in community practices.

## Acknowledgments

Supported by grant NIH RO1-EY013178-8 from the National Institutes of Health, Bethesda, Maryland.

The authors thank Hiroshi Ishikawa, MD, for his assistance.

## REFERENCES

- Huang D, Swanson EA, Lin CP, et al. Optical coherence tomography. *Science* 1991;254:1178–1181. [PubMed: 1957169]
- Salvini C, Massi D, Cappetti A, et al. Application of optical coherence tomography in non-invasive characterization of skin vascular lesions. *Skin Res Technol* 2008;14:89–92. [PubMed: 18211606]
- Jang IK, Bouma BE, Kang DH, et al. Visualization of coronary atherosclerotic plaques in patients using optical coherence tomography: comparison with intravascular ultrasound. *J Am Coll Cardiol* 2002;39:604–609. [PubMed: 11849858]
- Hee MR, Izatt JA, Swanson EA, et al. Optical coherence tomography of the human retina. *Arch Ophthalmol* 1995;113:325–332. [PubMed: 7887846]
- Puliafita CA, Hee MR, Lin CP, et al. Imaging of macular diseases with optical coherence tomography. *Ophthalmology* 1995;102:217–229. [PubMed: 7862410]
- Morgner U, Drexler W, Kartner FX, et al. Spectroscopic optical coherence tomography. *Opt Lett* 2000;25:111–113. [PubMed: 18059799]
- Wojtkowski M, Kowalczyk A, Leitgeb R, Fercher AF. Full range complex spectral optical coherence tomography technique in eye imaging. *Opt Lett* 2002;27:1415–1417. [PubMed: 18026464]
- Ko TH, Fujimoto JG, Schuman JS, et al. Comparison of ultrahigh- and standard-resolution optical coherence tomography for imaging macular pathology. *Ophthalmology* 2005;112:1922.e1–1922.e15. [PubMed: 16183127]
- Srinivasan VJ, Wojtkowski M, Witkin AJ, et al. High-definition and 3-dimensional imaging of macular pathologies with high-speed ultrahigh-resolution optical coherence tomography. *Ophthalmology* 2006;113:2054. [PubMed: 17074565]
- Schocket LS, Witkin AJ, Fujimoto JG, et al. Ultrahigh-resolution optical coherence tomography in patients with decreased visual acuity after retinal detachment repair. *Ophthalmology* 2006;113:666–672. [PubMed: 16581427]
- Hangai M, Ojima Y, Gotoh N, et al. Three-dimensional imaging of macular holes with high-speed optical coherence tomography. *Ophthalmology* 2007;114:763–773. [PubMed: 17187861]

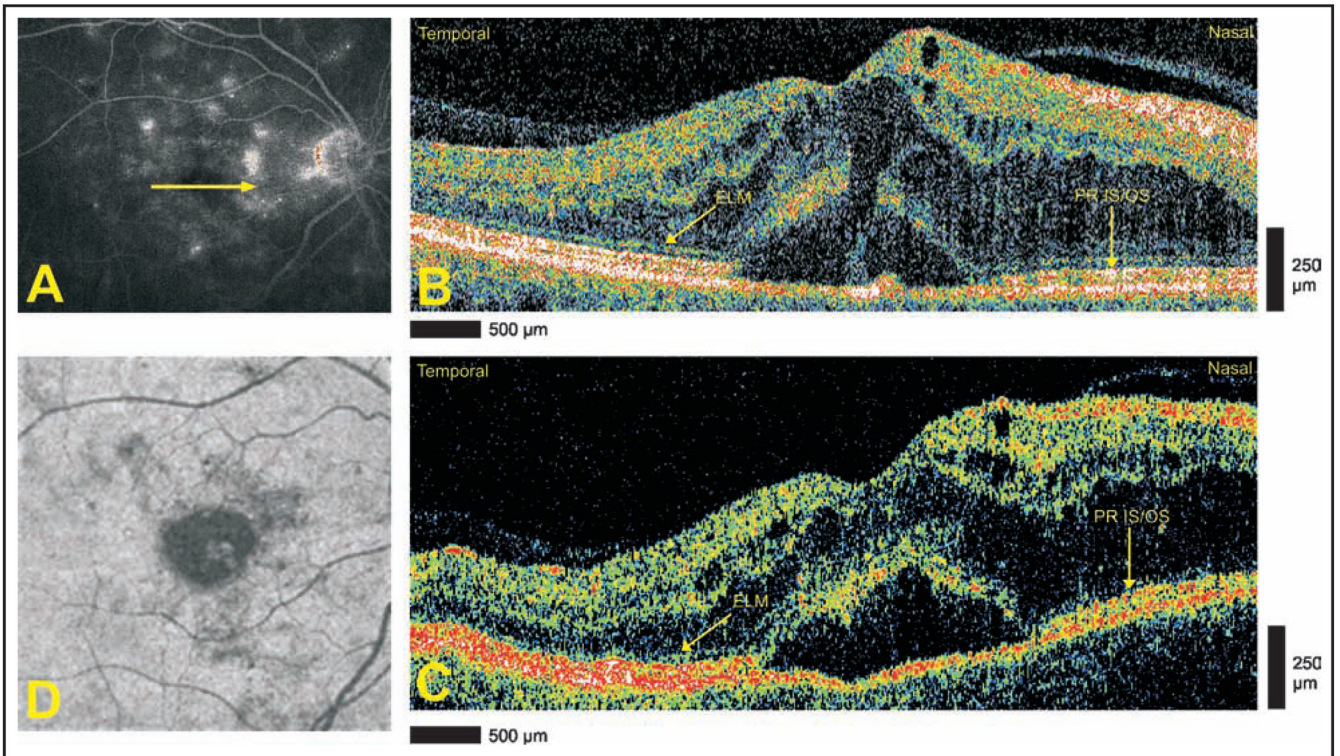


**Figure 1.**

Diabetic maculopathy and serous retinal detachment. (A) Late-phase optomap *fa* fluorescein angiogram demonstrating diffuse leakage. Arrow depicts direction of optical coherence tomography scans. (B) Cirrus HD-OCT (Carl Zeiss Meditec, Dublin, CA) and (C) StratusOCT (Carl Zeiss Meditec) images, respectively, demonstrating the intact external limiting membrane (ELM) temporally and the photoreceptor inner segment/outer segment (PR IS/OS) nasally. The sensory retina in the area of detachment is blurred, and the continuity of the ELM and PR IS/OS is not appreciated. (D) Advanced visualization C-scan image using a retinal pigment epithelium-aligned contour over a 53- $\mu$ m thickness centered above the retinal pigment epithelium. The area of serous retinal detachment is seen as a low-reflectivity spot in the surrounding high-reflectivity areas.

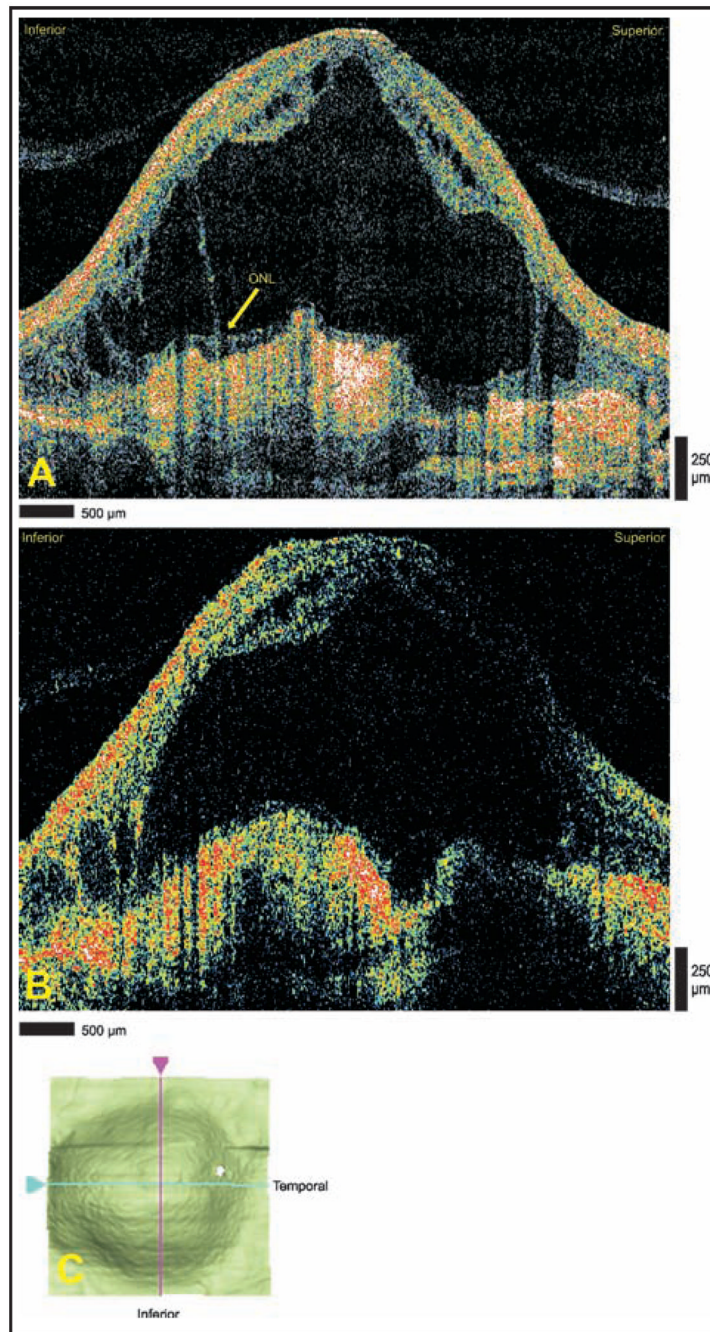


**Figure 2.**

Massive subretinal fluid due to exudative age-related macular degeneration. (A) Cirrus HD-OCT (Carl Zeiss Meditec, Dublin, CA) and (B) StratusOCT (Carl Zeiss Meditec) images demonstrating a large subretinal fluid accumulation overlying disciform scarring. The Cirrus HD-OCT image shows a portion of the outer plexiform layer (OPL) remaining adjacent to the scarred area. Note the finer detail of the cystoid structures displayed in the Cirrus HD-OCT image. (C) Interactive internal limiting membrane segmentation data map demonstrating the two-dimensional area of internal limiting membrane elevation. ONL = outer nuclear layer.



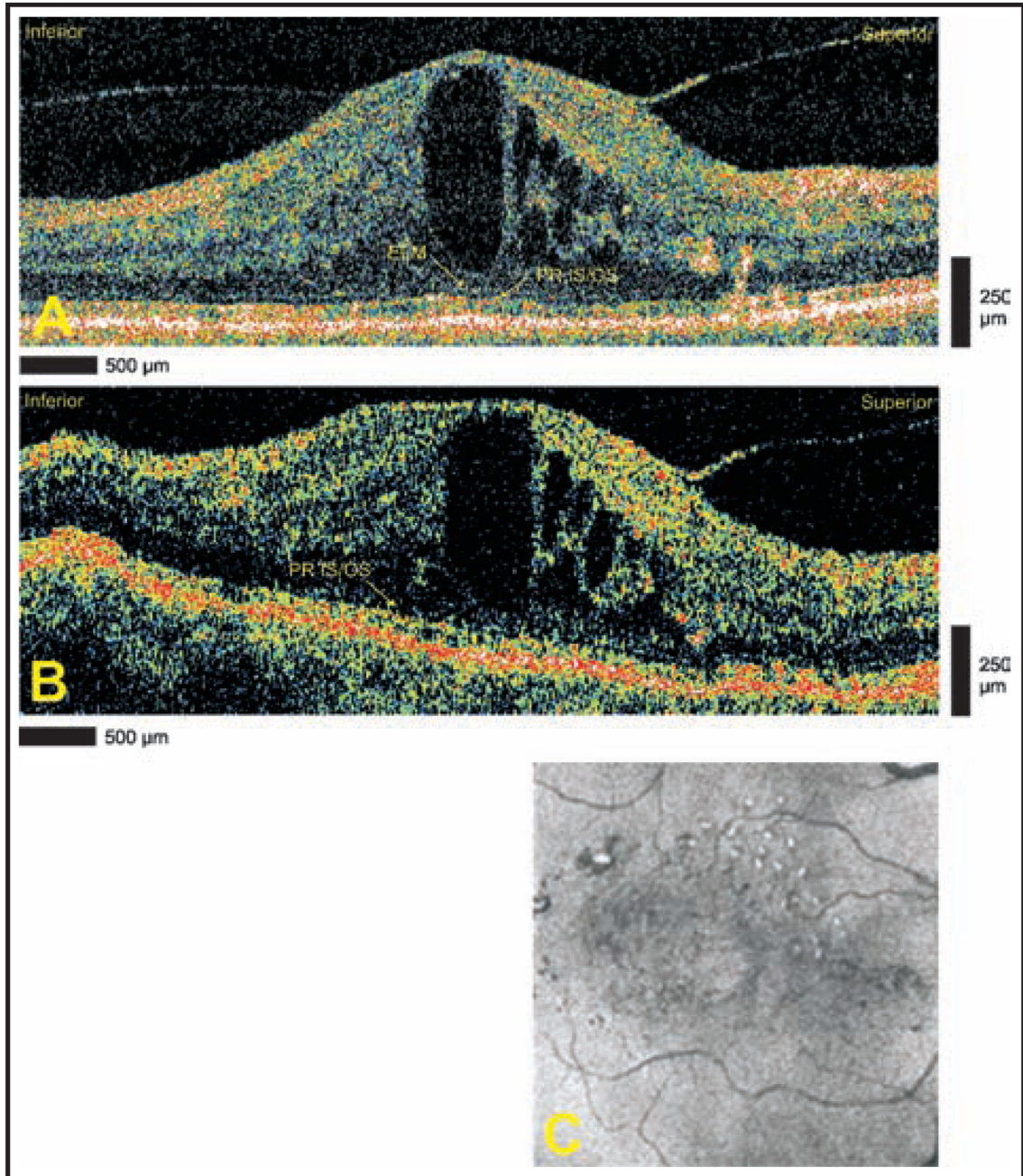


**Figure 3.**

Diabetic macular edema. (A) Cirrus HD-OCT (Carl Zeiss Meditec, Dublin, CA) and (B) StratusOCT (Carl Zeiss Meditec) images demonstrating cystoid edema. The Cirrus HD-OCT image demonstrates the continuity of the external limiting membrane (ELM) and the photoreceptor inner segment/outer segment (PR IS/OS) through the fovea. The ELM is not clearly seen in the StratusOCT image. (C) Advanced visualization C-scan image using a retinal pigment epithelium-aligned contour over a 53- $\mu$ m thickness centered above the retinal pigment epithelium. Hard exudates are seen superiorly.

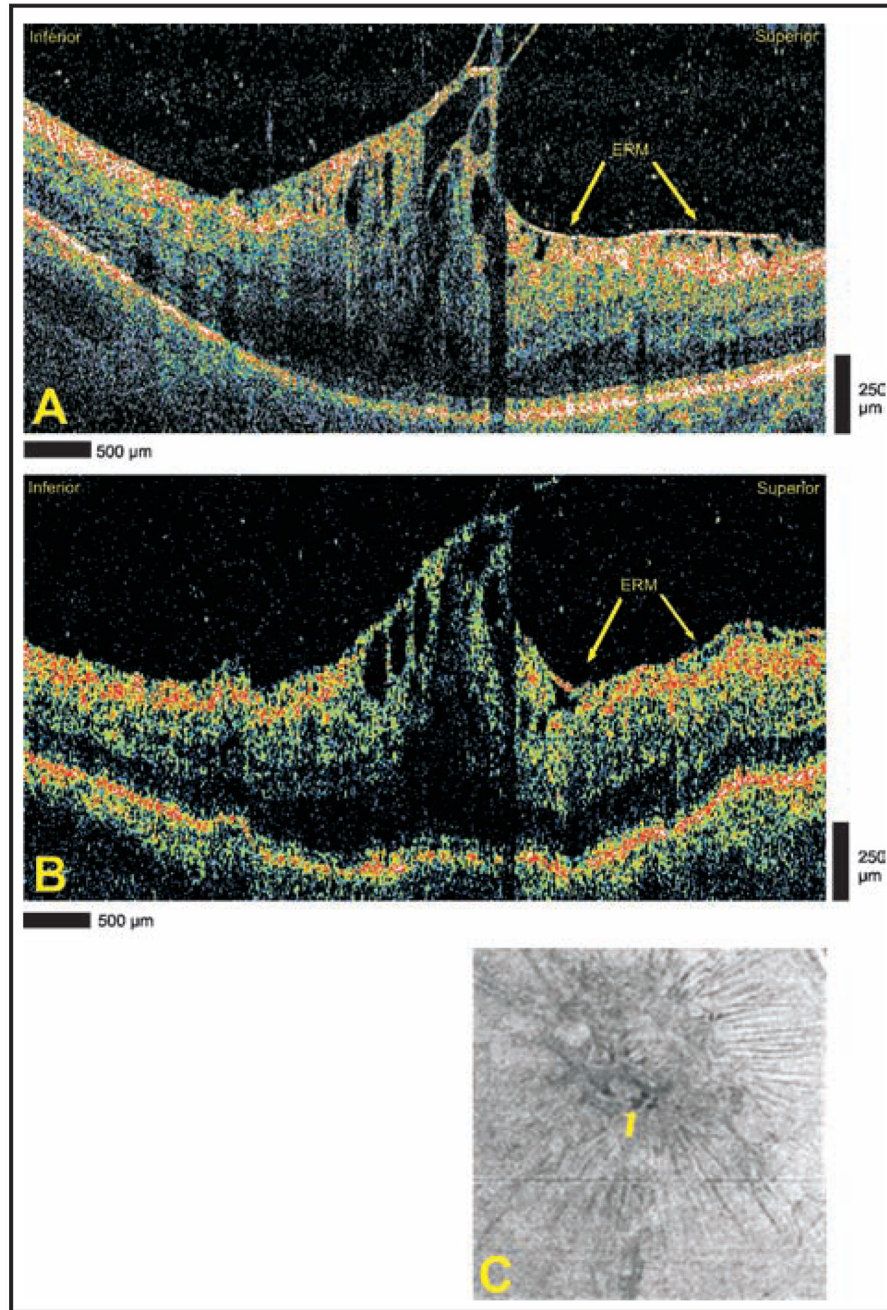


**Figure 4.** Severe vitreomacular traction. (A) Cirrus HD-OCT (Carl Zeiss Meditec, Dublin, CA) and (B) StratusOCT (Carl Zeiss Meditec) images demonstrating vitreomacular traction and foveal cysts. An epiretinal membrane (ERM) is identified in both images. (C) Advanced visualization C-scan image using an internal limiting membrane-aligned contour over a 39-µm thickness centered at the internal limiting membrane. The arrow designates the location of foveal cysts.



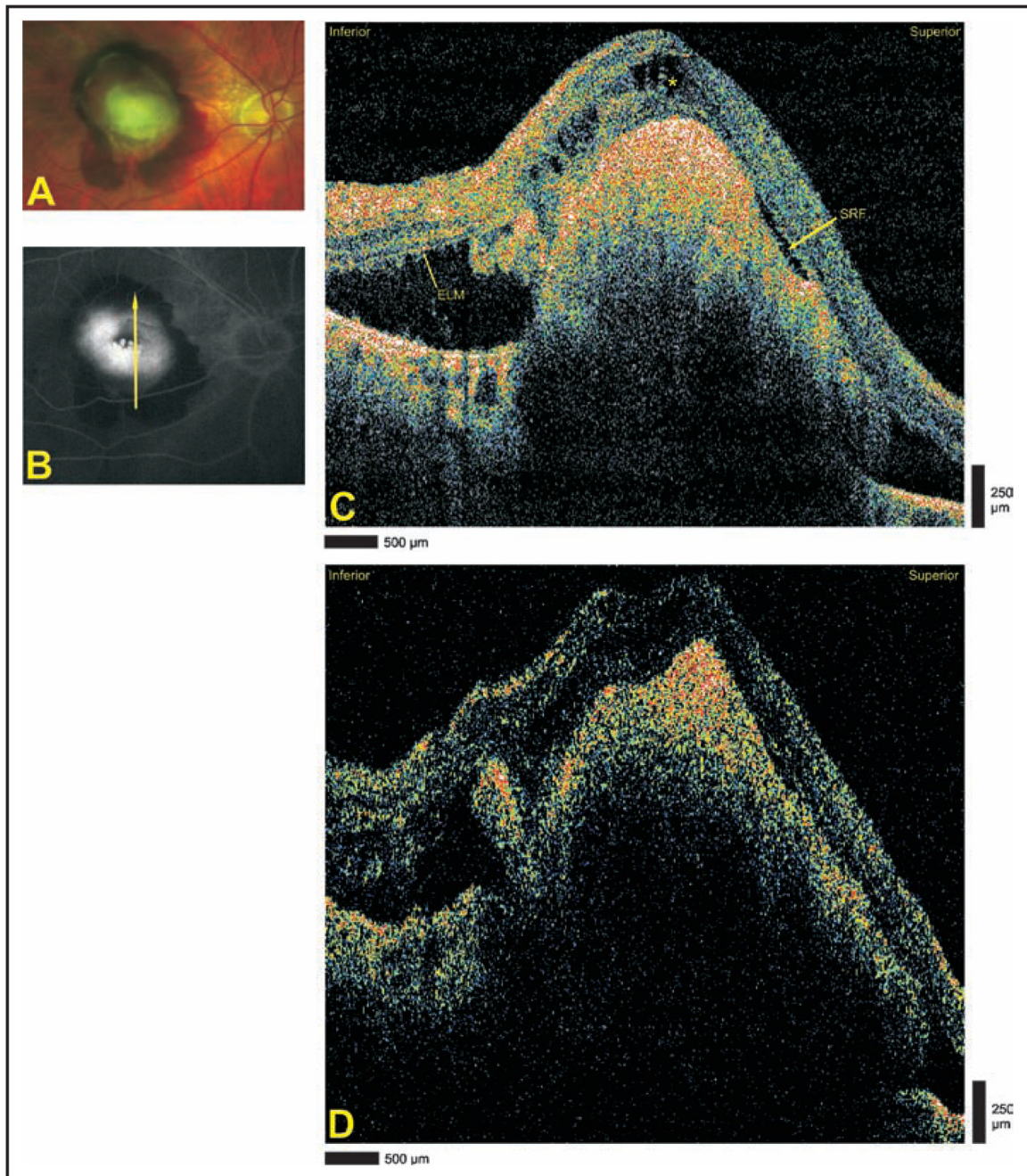


**Figure 5.**

Extensive choroidal neovascularization due to exudative age-related macular degeneration. (A) Optomap *fa* fundus photograph demonstrating subretinal hemorrhage. (B) Late-phase optomap *fa* fluorescein angiography demonstrating central hyperfluorescence surrounded by blockage by hemorrhage. Arrow depicts direction of optical coherence tomography scans. (C) Cirrus HD-OCT (Carl Zeiss Meditec, Dublin, CA) and (D) StratusOCT (Carl Zeiss Meditec) images demonstrating extensive choroidal neovascularization and subretinal hemorrhage. Superiorly, a small pocket of subretinal fluid (SRF) is identified in the Cirrus HD-OCT image, and the external limiting membrane (ELM) is seen in the inferior portion of the image. The asterisk designates cystoid edema.



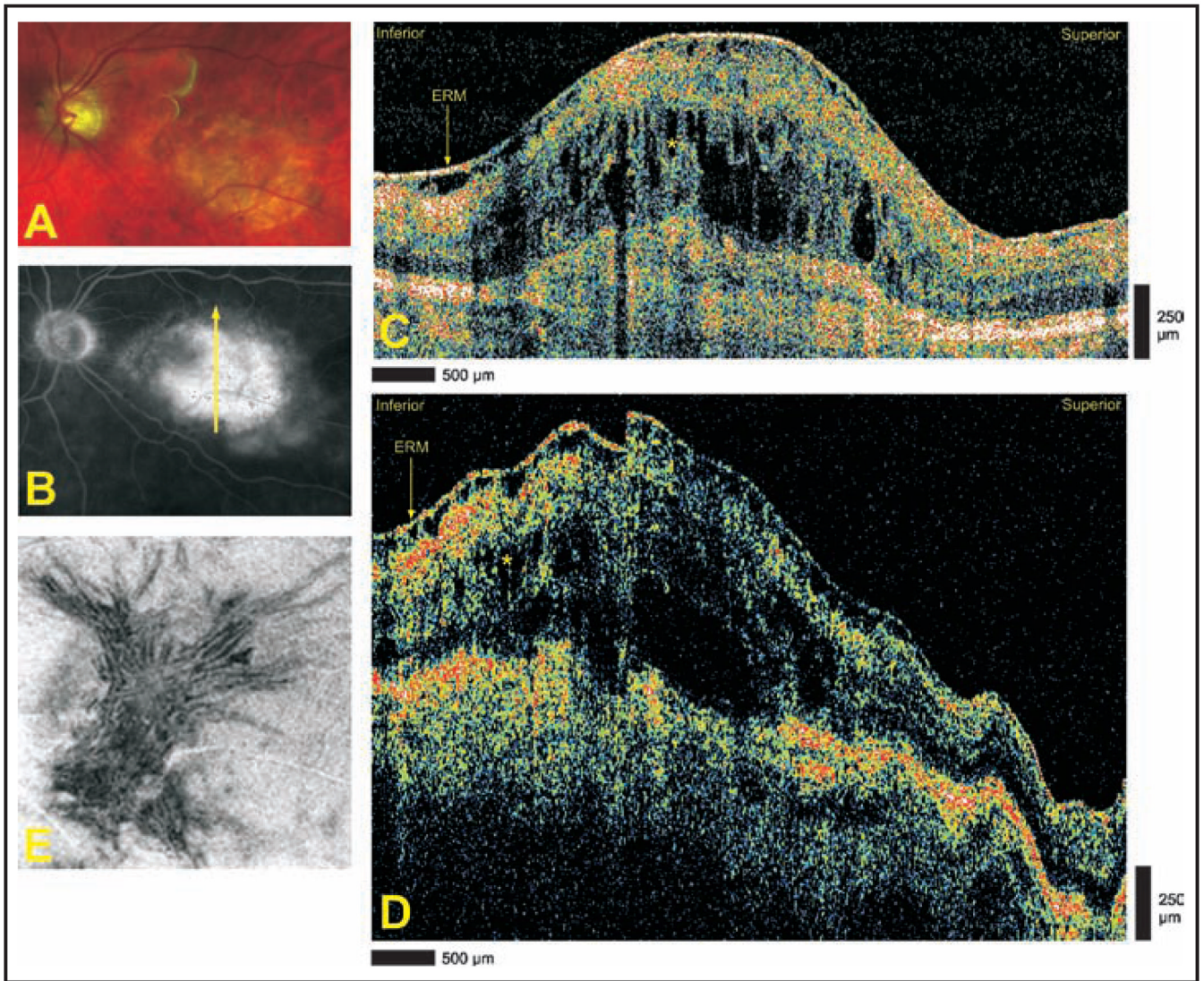


**Figure 6.**

Exudative age-related macular degeneration with disciform scar. (A) Optomap *fa* fundus photograph demonstrating central disciform scar with subretinal fluid and faint hemorrhage. (B) Late-phase optomap *fa* fluorescein angiogram demonstrating a central area of hyperfluorescence. Arrow depicts direction of optical coherence tomography scans. (C) Cirrus HD-OCT (Carl Zeiss Meditec, Dublin, CA) and (D) StratusOCT (Carl Zeiss Meditec) images demonstrating extensive epiretinal membrane (ERM), cystoid edema (asterisks), and scarring. (E) Advanced visualization C-scan image using an internal limiting membrane-aligned contour over a 35- $\mu$ m thickness centered at the internal limiting membrane. Deep retinal folds are apparent throughout the image.